

Обзор ArXiv/astro-ph, начало октября 2021

От Сильченко О.К.

ArXiv: 2110.00408

The origin of star-gas misalignments in simulated galaxies

Catalina I. Casanueva,^{1,2*} Claudia del P. Lagos,^{3,4} Nelson D. Padilla^{1,2}, Thomas A. Davison^{5,6}

¹*Instituto de Astrofísica, Pontificia Universidad Católica de Chile, Av. Vicuña Mackenna 4860, Santiago, Chile*

²*Centro de Astro-Ingeniería, Pontificia Universidad Católica de Chile, Av. Vicuña Mackenna 4860, Santiago, Chile*

³*International Centre for Radio Astronomy Research (ICRAR), M468, University of Western Australia, 35 Stirling Hwy, Crawley, WA 6009, Australia*

⁴*Australian Research Council Centre of Excellence for All-sky Astrophysics (CAASTRO), 44 Rosehill Street Redfern, NSW 2016, Australia*

⁵*Jeremiah Horrocks Institute, University of Central Lancashire, Preston PR1 2HE, UK*

⁶*European Southern Observatory, Karl-Schwarzschild-Strasse 2, D-87548 Garching bei Muenchen, Germany*

Accepted XXX. Received YYY; in original form ZZZ

ABSTRACT

We study the origin of misalignments between the stellar and star-forming gas components of simulated galaxies in the EAGLE simulations. We focus on galaxies with stellar masses $\geq 10^9 M_{\odot}$ at $0 \leq z \leq 1$. We compare the frequency of misalignments with observational results from the SAMI survey and find that overall, EAGLE can reproduce the incidence of misalignments in the field and clusters, as well as the dependence on stellar mass and optical colour within the uncertainties. We study the dependence on kinematic misalignments with internal galaxy properties and different processes related to galaxy mergers and sudden changes in stellar and star-forming gas mass. We found that despite the environment being relevant in setting the conditions to misalign the star-forming gas, the internal galaxy properties play a crucial role in determining whether the gas quickly aligns with the stellar component or not. Hence, galaxies that are more triaxial and more dispersion dominated display more misalignments because they are inefficient at realigning the star-forming gas towards the stellar angular momentum vector.

Simulations EAGLE: куб 100 Мpc, 4 миллиарда частиц, разрешение 0.7 кпк и 0.3-1.0 млрд лет

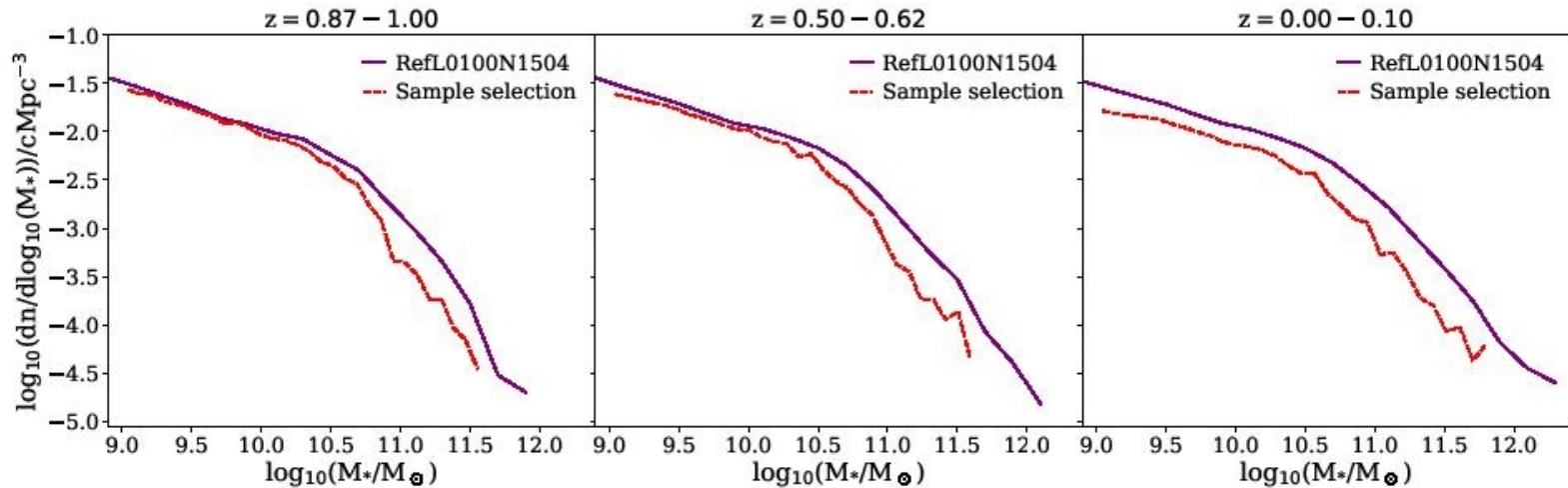


Figure 1. Stellar mass function of all galaxies in the RefL0100N1504 simulation (solid purple lines) in comparison with our sample selection (dashed red lines), at the three redshift ranges as labelled in each panel.

Свойства галактик:

- Масса, <70 крс
- $sSFR$, <70 крс
- Масса (доля) звездообразующего газа
- Доля со-вращающейся кинетической энергии звезд (→ вклад балджа и диска)
- Триаксиальность
- Анизотропия дисперсии скоростей звезд
- Отношение дисперсии скоростей звезд к скорости вращения
- Процессы: слияния
- Процессы: резкий рост/падение массы звезд и/или газа

Сравнение с SAMI: окружение

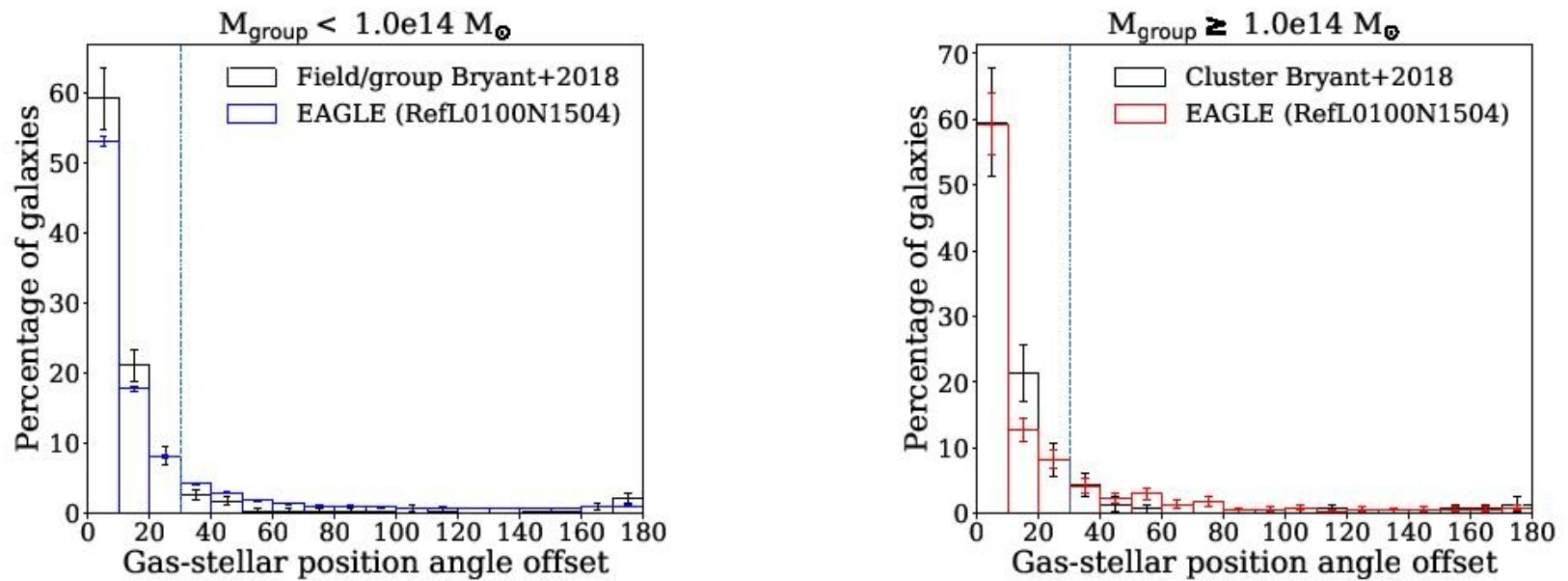


Figure 2. Distribution of the angles between the rotation axis of the stars and star-forming gas for galaxies that reside in groups of mass $< 10^{14} M_{\odot}$ (left) and galaxies that reside in groups of mass $> 10^{14} M_{\odot}$ (right). Blue dotted lines mark a PA offset = 30° to separate between aligned and misaligned galaxies. Dotted and solid histograms show the distribution for galaxies in SAMI (Bryant et al. 2018) and EAGLE, respectively. Error bars in the EAGLE simulations show Poisson errors.

Сравнение с SAMI: масса и цвет

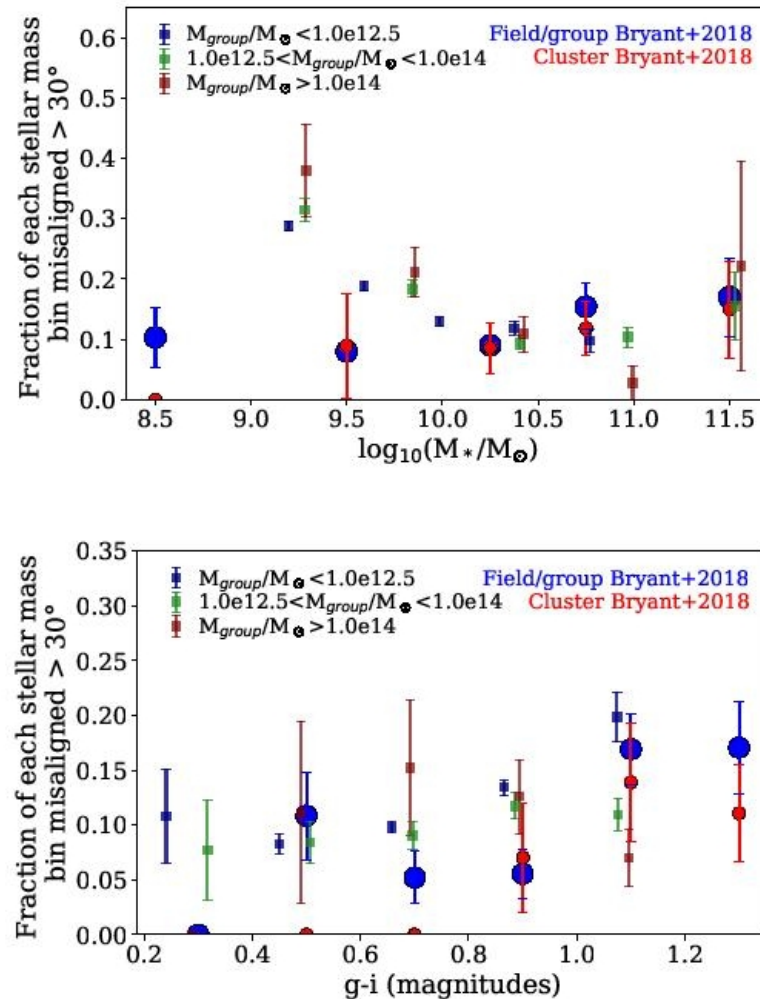


Figure 3. Fraction of galaxies that are misaligned (PA offset > 30°) in bins of

Антикорреляция с темпом звездообразования

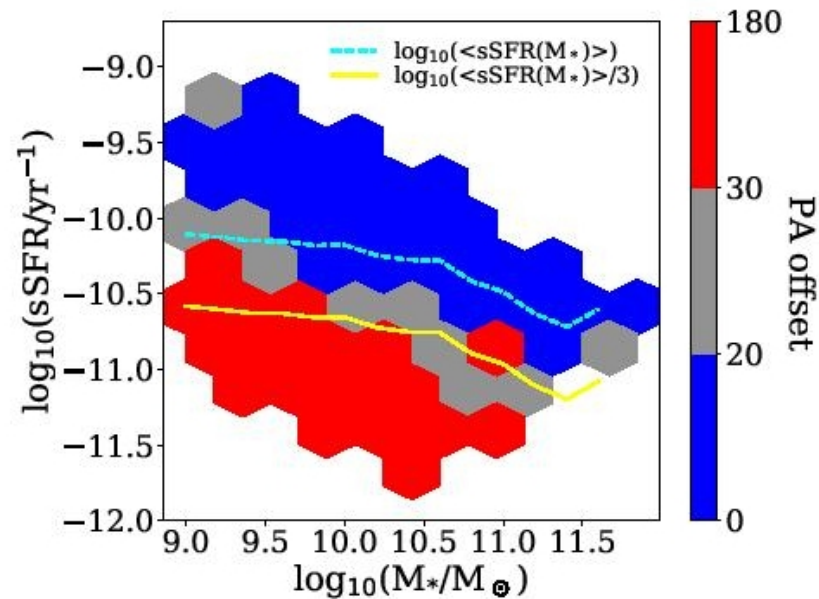


Figure 8. Binned distribution of galaxies in the $\text{sSFR}-M_*$ plane coloured by the average gas-stellar position angle offset at $z = 0.0-0.11$. The dashed blue line marks the main sequence of star formation and solid yellow line separates the population between blue cloud and red sequence. Only bins with more than five galaxies are shown.

Эволюция рассогласования вращения газа и звезд

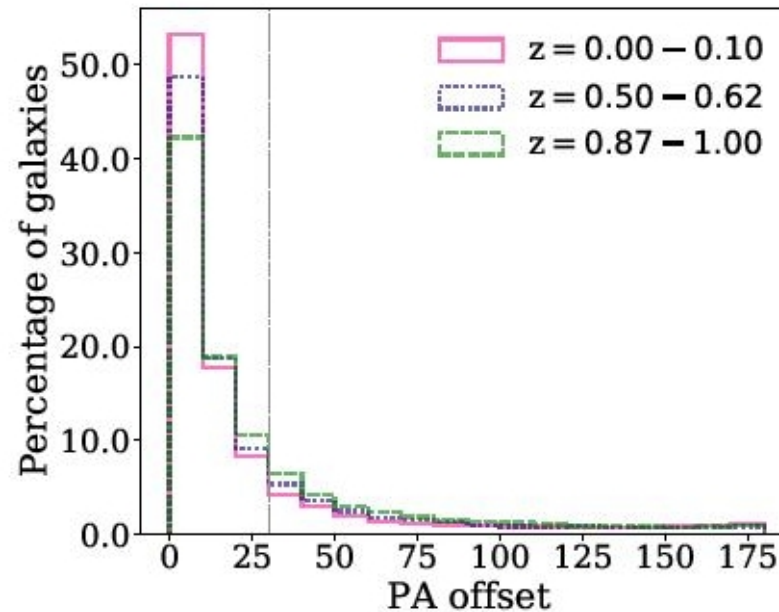


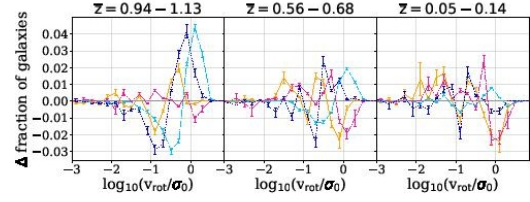
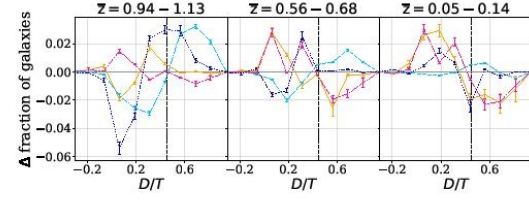
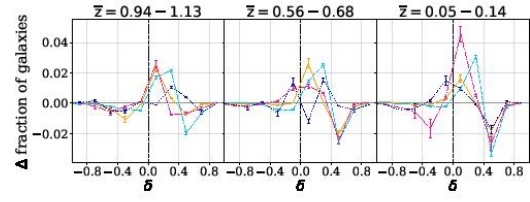
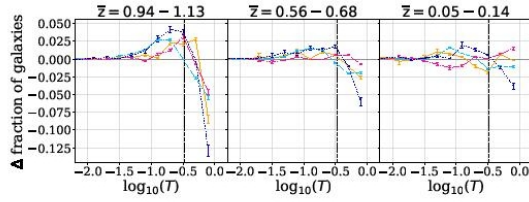
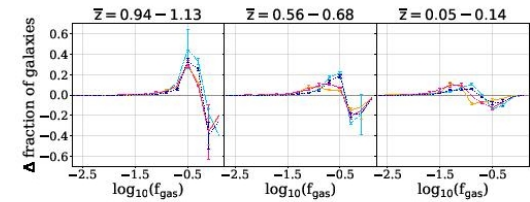
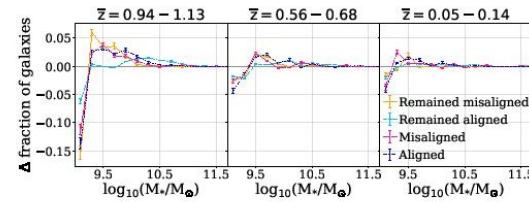
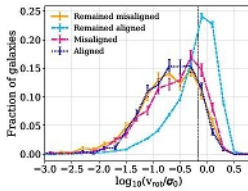
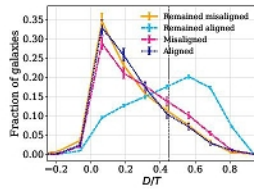
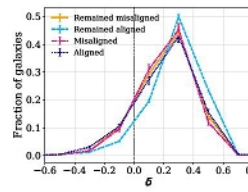
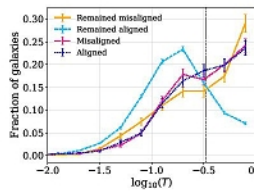
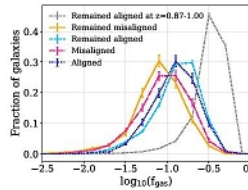
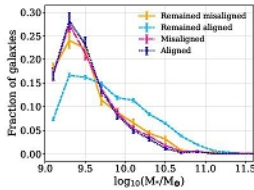
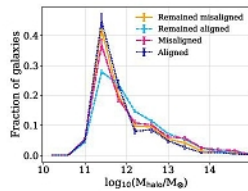
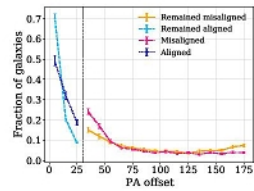
Figure 5. Distribution of the angles between the rotation axis of the stars and star-forming gas for galaxies at the three redshift ranges, as labelled. The grey dashed line marks PA offset = 30° to separate between aligned and misaligned galaxies.

Как долго может держаться рассогласование?

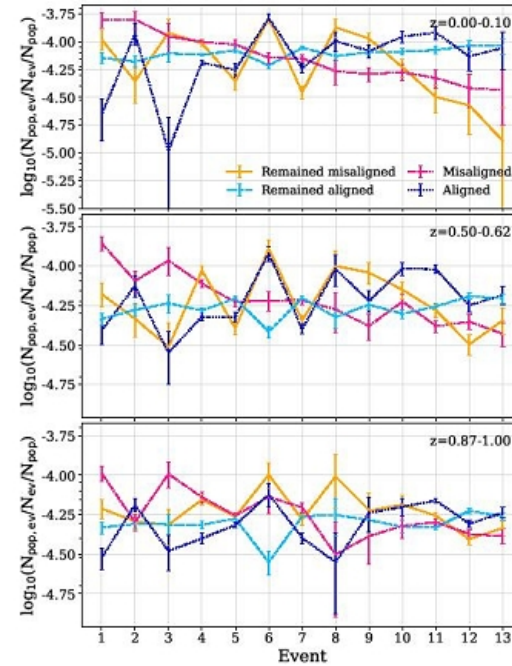
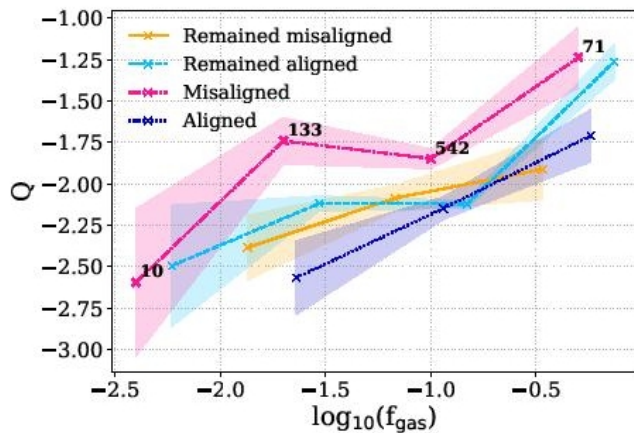
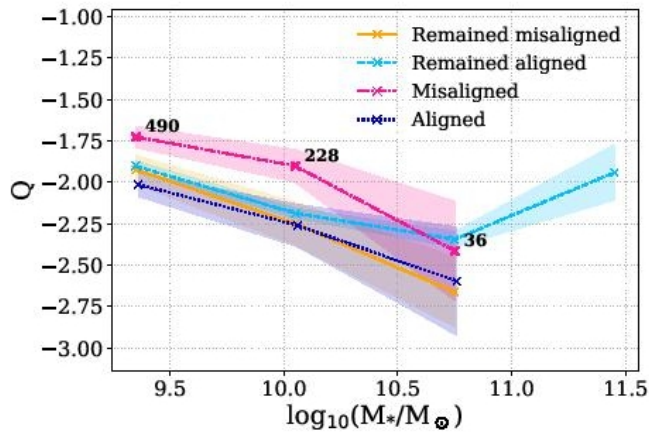
Population label	Description	Number of galaxies		
		$z = 0.87 - 1.00$	$z = 0.50 - 0.62$	$z = 0.00 - 0.10$
Remained misaligned	Galaxies that were and remain misaligned since the previous snapshot.	2409 (11±0.2%)	1413 (7±0.2%)	990 (6±0.2%)
Remained aligned	Galaxies that are aligned and remain so in two consecutive snapshots.	11375 (56±0.6%)	13205 (69±0.7%)	12037 (76±0.9%)
Misaligned	Galaxies that become misaligned between consecutive snapshots.	2605 (12±0.2%)	2159 (11±0.2%)	1474 (9±0.2%)
Aligned	Galaxies that were misaligned in the previous snapshot and become aligned in the present one.	3886 (19±0.3%)	2163 (11±0.2%)	1266 (8±0.2%)

Table 1. Description of the populations analysed in Section 3.2.2. The number of galaxies and the percentage of galaxies of each population is tabulated for each redshift range. This sample is limited to galaxies that meet the selection described in Section 2.1 for two consecutive snapshots.

Сравнение частоты явления с внутренними свойствами галактик



Но источник газа должен быть внешний??



- | | |
|--|---|
| 1 - M_* and $M_{\text{SF}} \downarrow 10\%$ | 8 - $M_{\text{SF}} \uparrow 5\%$ |
| 2 - Merger ratio > 0.1 | 9 - Unidentified |
| 3 - $M_{\text{SF}} \downarrow 10\%$ and $M_* \downarrow 5\%$ | 10 - $M_{\text{SF}} \uparrow 10\%$ and $M_* \uparrow 5\%$ |
| 4 - $M_{\text{SF}} \downarrow 10\%$ | 11 - M_* and $M_{\text{SF}} \uparrow 10\%$ |
| 5 - $M_{\text{SF}} \downarrow 10\%$ and $M_* \uparrow 10\%$ | 12 - $M_* \uparrow 10\%$ |
| 6 - $M_{\text{SF}} \uparrow 10\%$ | 13 - $M_{\text{SF}} \uparrow 5\%$ and $M_* \uparrow 10\%$ |
| 7 - $M_{\text{SF}} \downarrow 10\%$ and $M_* \uparrow 5\%$ | |

Figure 15. Number of galaxies of each population associated with an event ($N_{\text{pop, ev}}$), over the total number of galaxies that experienced that event (N_{ev}), and over the total number of galaxies in that population (N_{pop}), at three redshift ranges (as labelled on each panel). The integers on the x-axis correspond to each event listed below the figure. Error bars are Poisson errors.

Апофеоз: галактики с рассогласованным вращением имеют строго тот же набор событий в жизни, что и нормальные

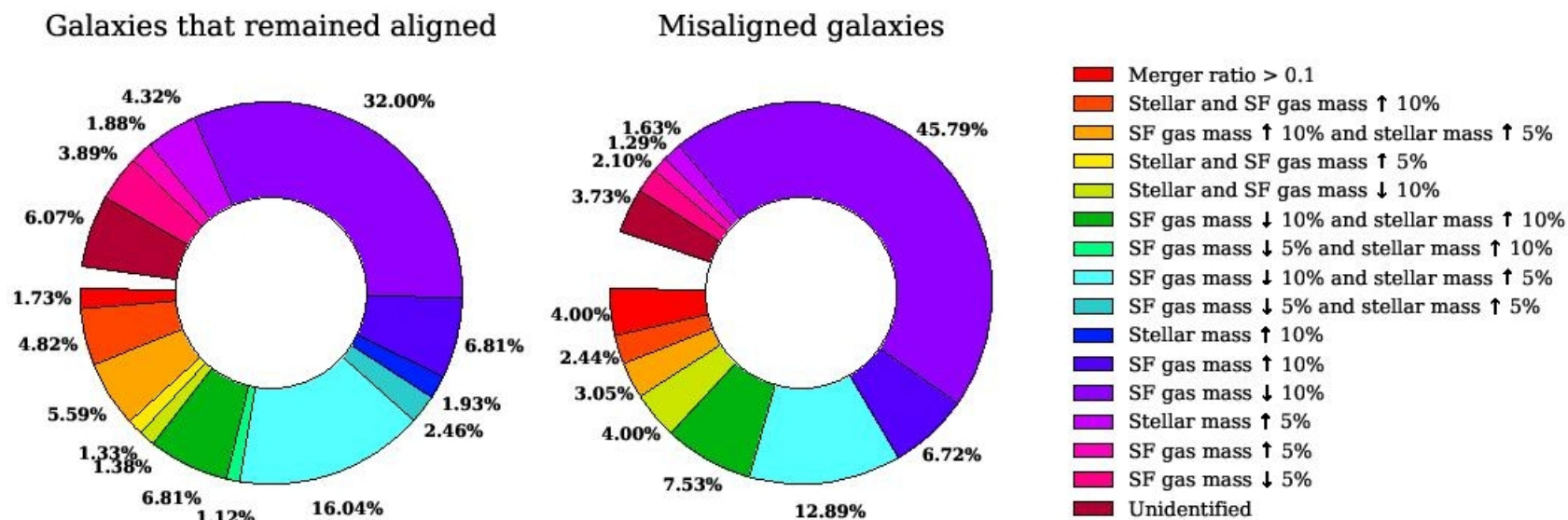


Figure 14. Each pie chart shows the fraction of galaxies of each population (as labelled) at $z=0.0-0.1$ that suffered a certain event in the previous snapshot. ↑ 5% and ↑ 10% mean increases between 5 and 10% and $\geq 10\%$, respectively. In these pie charts, we only show events that occurred in more than 1% of the galaxies of each population.